
Proceedings Paper:
Shen, Lu, Henson, Benjamin and Zakharov, Yury (2022) Full-Duplex UWA Communication System with Two Iterations. In: Sixth Underwater Communications and Networking Conference. 2022 Sixth Underwater Communications and Networking Conference (UComms). IEEE, pp. 1-5.

https://doi.org/10.1109/UComms56954.2022.9905675

Full-Duplex UWA Communication System with Two Iterations

Lu Shen, Benjamin Henson, Yuriy Zakharov
Department of Electronic Engineering, University of York, UK

***Abstract*—We consider full-duplex (FD) underwater acoustic (UWA) systems when the transceiver simultaneously transmits and receives in the same frequency bandwidth. The major task of the FD operation is to cancel the strong self-interference (SI) from the near-end projector. Advanced adaptive filtering algorithms have been proposed previously, capable of providing high-accuracy SI channel estimates even in scenarios with fast SI channel variations. A high level of SI cancellation can be achieved when the far-end signal is absent. However, the SI channel estimation performance is limited in FD scenarios as the far-end signal is treated as interference when estimating the near-end SI channel thus increasing the noise floor. In this paper, we propose a new FD UWA system which alternates between the near-end SI cancellation and far-end data demodulation. The FD UWA system performance is evaluated in a lake experiment using a recently developed two-element transducer. Results show 2 dB loss in the detection performance of the FD system compared to the corresponding half-duplex system in the same lake experiment.**

***Index Terms*—Adaptive filter, Channel estimation, Full-duplex, Rake receiver, Self-interference cancellation, Underwater acoustics.**

I. Introduction

Underwater acoustic (UWA) communication suffers from limited bandwidth for data transmission as attenuation increases with signal frequency [1]. To increase the spectral efficiency within the available frequency bandwidth, we consider full-duplex (FD) operation, which allows simultaneous transmission and reception in the same frequency bandwidth [2]–[5]. The major problem in implementing FD systems is to cancel the strong self-interference (SI) signal from the near-end projector. A high level of SI cancellation (SIC) is required to detect the weak far-end signal. For FD terrestrial radio communications, a combination of analogue and digital cancellation is normally used to avoid the analogue-to-digital converter (ADC) saturation [2]–[4]. For FD UWA systems, lower-frequency acoustic signals are transmitted. In such a case, high resolution ADCs up to 24 bits can be used, which makes it feasible to perform digital cancellation without ADC saturation. Therefore, digital cancellation is considered as the main approach of SIC in FD UWA systems [6]–[9].

In previous works, it is found that the digital SIC performance in FD UWA systems is limited by two main factors, the first one is the nonlinearities introduced by the equipment [6], [10], [11] and the second one is the fast variation of the SI channel [8], [9]. The dominant source of the nonlinearities in the FD system comes from the power amplifier (PA). It is found that the SIC performance can be significantly improved by using the PA output as the reference signal (regressor) compared to the case of using the original digital data [10], [12]. With that taken into account, a high level of digital SIC can be achieved in time-invariant scenarios with a classical recursive least-squares (RLS) adaptive filter [13]. In practice, the SI channel can be fast time-varying predominantly due to reflections from the moving sea surface. To achieve a high level of digital SIC in time-varying scenarios, advanced adaptive filtering algorithms with good tracking performance have been proposed [8], [9]. The SIC achieved using these adaptive algorithms have been evaluated in shallow lake experiments. However, in those experiments, the far-end transmission is not considered and the SIC is limited by the noise level.

With FD operations, the received signal includes the near-end SI, background noise, and also the far-end signal. To achieve a high level of digital SIC, the influence of the far-end signal, in addition to the noise, on the SIC performance must be taken into account. When we estimate the near-end SI channel, the far-end signal is treated as an additional interference (noise), which reduces the overall SI to noise ratio. Therefore, the higher far-end signal to noise ratio (SNR), the poorer the SIC performance. To address the impact of the far-end signal on the SIC performance, we propose a new FD UWA system which performs SIC and far-end data demodulation in two iterations. In the first iteration, the SI channel is estimated, treating the far-end signal as an extra noise in the same way as described in [8], [9], by an adaptive filter. The next step is the far-end channel estimation using the known pilot transmitted by the far-end and the residual signal after the first SIC iteration. Since the far-end channel is multipath, the Rake receiver [14] is used for detection of the far-end signal. In the second iteration, we reconstruct the far-end signal using the far-end data estimates from the first iteration and remove it from the received signal to perform the second iteration of digital SIC. After that, new far-end data estimates are obtained in the same way as in the first iteration. As the estimation performance for both the near-end SI channel and far-end channel is significantly improved in the second iteration, a better demodulation performance can be achieved. To evaluate the performance of the FD UWA system, lake experiments are conducted using the recently developed two-element transducers. Both half-duplex and FD communication experiments are conducted for the performance comparison. Results indicate that the second iteration significantly improves the demodulation performance. With a rate 1/4 convolutional

The work of L. Shen, B. Henson and Y. Zakharov was supported in part by the U.K. EPSRC through Grants EP/P017975/1 and EP/R003297/1.

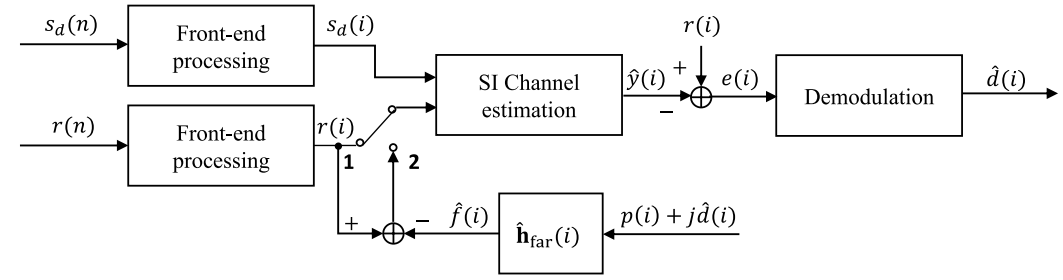

(a) FD UWA system structure.

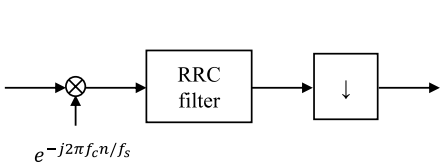

(b) Front-end processing block.

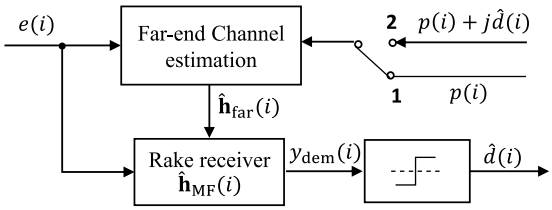

(c) Demodulation block.

Fig. 1: Block diagrams of the FD UWA system. The system works at two sampling rates. The sample index with the high sampling rate f_s and symbol rate f_d are denoted by n and i, respectively; $s_d(i)$ and $r(i)$ represent the baseband PA output and hydrophone output, respectively; $\hat{y}(i)$ is an estimate of the SI signal, $e(i)$ is the residual signal after SIC, $\hat{f}(i)$ is the far-end signal estimate, $p(i)$ is the pilot signal used in the far-end transmission. Switch between 1 and 2 represents the choice of input signals in the first and second iterations, respectively.

code, the SNR performance loss in the FD experiment is less than 2 dB compared to the half-duplex case.

II. System model

In Subsection II-A describes signals used for near-end and far-end transmission. Subsection II-B introduces the FD UWA system structure.

A. Transmitted signal

For the near-end transmission, a pseudo-random sequence of Binary Phase Shift Keying (BPSK) data symbols are used. The transmitted data is up-sampled and pulse-shaped by a root-raised cosine (RRC) filter. The RRC filter output is then up-converted to the carrier frequency f_c. Afterwards, the signal is digital-to-analogue converted, amplified by a PA and transmitted by a projector.

For the far-end transmission, Quadrature Phase Shift Keying (QPSK) symbols consisting of superimposed binary pilot and data symbols [15], [16] are used:

$$D(i) = p(i) + jd(i), \tag{1}$$

where $p(i)$ is a binary pseudo-random pilot sequence and $d(i)$ is the information data symbols obtained by interleaving and encoding transmitted data using a convolutional code.

B. FD UWA system design

The FD UWA system model is shown in Fig. 1. The system works at two sampling rates. The high sampling rate f_s is applied to the signal received by the hydrophone. The low sampling rate f_d is used for SI and far-end channel estimation. The FD system has two tasks, the first task is to perform the near-end SI cancellation, and the second task is to perform the far-end data demodulation. In this paper, we consider static transmitter and receiver. The Doppler effect (channel variation) is dealt with by the channel estimation blocks.

An adaptive filter is used for the near-end SIC. It works at the symbol rate f_d to avoid the ill-conditioning problem in the adaptive filter. To incorporate the nonlinearities introduced by the PA in the reference signal, we use the baseband digitalized PA output $s_d(i)$ as the regressor. The baseband hydrophone output $r(i)$ is used as the desired signal. The baseband signals are obtained using the front-end processing block as shown in Fig. 1 (b), where the RRC filter is used for low-pass filtering. After SI channel estimation, the estimate of the SI signal $\hat{y}(i)$ is subtracted from the received signal $r(i)$. The residual signal $e(i)$ is treated as an estimate of the far-end signal (plus noise) to proceed with the far-end data demodulation.

The demodulation process is illustrated in Fig. 1 (c). The time synchronisation for the far-end transmission is done in the far-end channel estimator by cross-correlation of the received signal and the pilot signal. The far-end channel estimates are obtained by another adaptive filter. The residual signal $e(i)$ after SIC is used as the desired signal of the adaptive filter. For the first iteration, we use the known pilot sequence as the reference signal (regressor). The far-end channel estimates $\hat{\mathbf{h}}_{\text{far}}(i)$ are then fed to a Rake receiver. The Rake receiver is implemented as a matched filter. The filter impulse response vector $\hat{\mathbf{h}}_{\text{MF}}(i)$ is the complex conjugate of the time-reversed version of the far-end channel estimate $\hat{\mathbf{h}}_{\text{far}}(i)$. The imaginary part of the Rake receiver output $y_{\text{dem}}(i)$ is used as the soft-

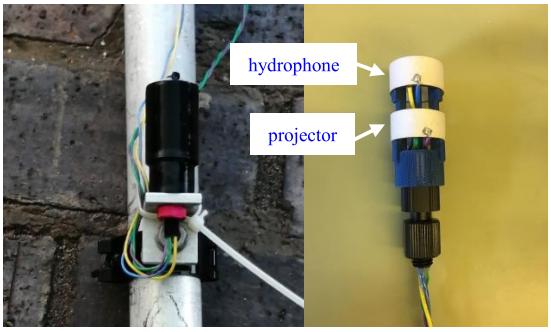

Fig. 2: A two-sensor transducer used in the lake experiments.

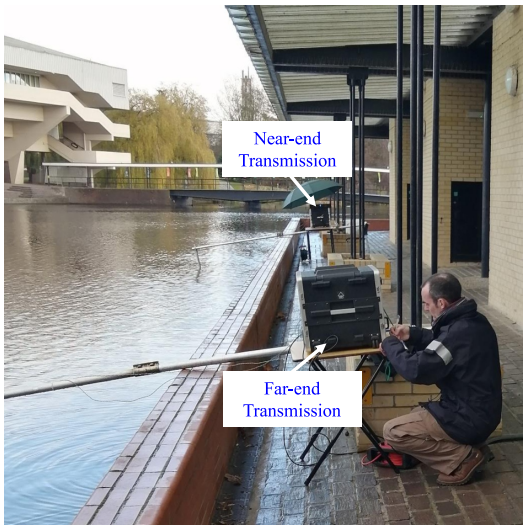

Fig. 3: Setup of the FD and half-duplex experiments.

decision of the far-end data symbol to which the Viterbi decoding [14] is applied.

At the second iteration, we try to improve the demodulation performance by eliminating the influence of the far-end signal on the SI channel estimation. The far-end symbol estimate $\hat{D}(i) = p(i) + j\hat{d}(i)$ is then recovered. An estimate of the far-end signal $\hat{f}(i)$ is then generated by filtering $\hat{D}(i)$ with the far-end channel estimates $\hat{\mathbf{h}}_{\text{far}}(i)$. At the second iteration, the residual signal $r(i) - \hat{f}(i)$ is used as the desired signal of the SI adaptive filter as shown in Fig. 1 (a). In such a case, the effect of the far-end signal on the SI channel estimation is significantly reduced. For the far-end channel estimation, $\hat{D}(i)$ is used as the regressor. The second iteration can significantly improve the demodulation performance as we obtain more accurate estimates of both the near-end and far-end channels.

III. Lake Experiment

In this section, we investigate the FD UWA system performance in lake experiments. Subsection III-A describes the experimental setup. Subsection III-B investigates the near-end SI and far-end channel estimation performance. The demodulation performance is presented in subsection III-C.

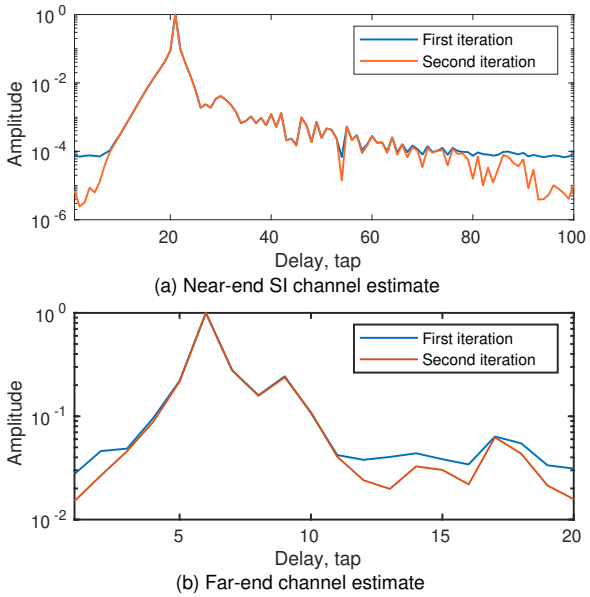

Fig. 4: Averaged amplitude of the impulse response estimates of the SI channel and far-end channel in the FD experiment.

A. Experimental setup

The lake experiments were conducted using the recently developed two-element transducer (see Fig. 2) which contains two piezo-ceramic cylinders, one of them is used as a projector and the other one is used as a hydrophone. Two of such transducers were used for near-end and far-end data transmission as shown in Fig. 3. During the experiment, both transducers were placed at approximately 0.5 m depth and the distance between them was around 18 m. The maximum depth of the experimental site is around 1 m.

For both the near-end and far-end transmission, the transmitted signal was sampled at $f_s = 192$ kHz. The RRC filter with a roll-off factor of 0.2 was used for pulse-shaping and low-pass filtering. For both experiments, we transmitted 65 s of signals including 5 s of silence period at the beginning to measure the background noise. As described in Section II, the near-end transmission used a BPSK signal at $f_c = 36$ kHz carrier frequency with 4 kHz bandwidth. From the far-end, the QPSK signal at the same carrier frequency and with the same bandwidth was transmitted. A rate 1/4 convolutional code is used, the constraint length is 8 and the code polynomials in octal are [235 275 313 357] [14]. Thus, the effective data rate is 1000 bits per second. Both half-duplex and FD experiments were conducted. For the half-duplex experiment, there was only the far-end transmission. The far-end SNR in both experiments was around 16 dB. For the FD experiment, the received SI signal to noise ratio was around 67 dB.

B. SI and far-end channel estimation

The first iteration of SIC does not require the use of advanced adaptive filters as the SIC performance is limited by the interference from the far-end signal. Therefore, we use

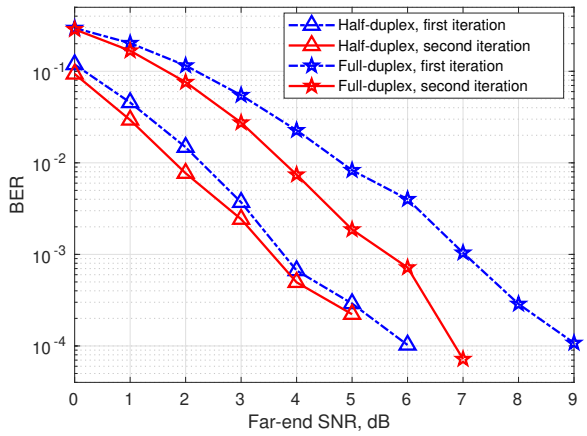

Fig. 5: BER performance of the receiver in the FD and half-duplex experiments.

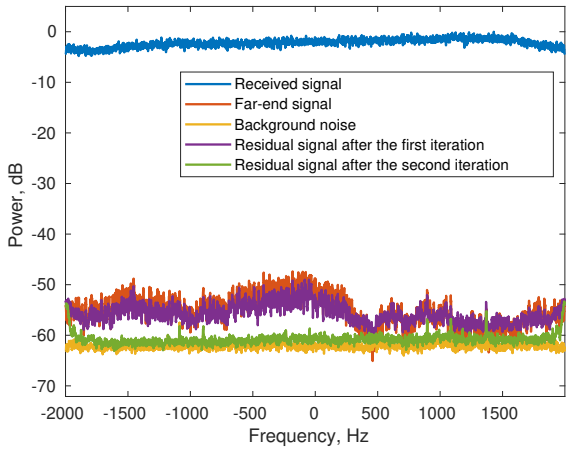

Fig. 6: Power spectra of the baseband signals in the lake experiments. The baseband far-end signal is obtained from the half-duplex experiment, the rest of the signals are obtained from the FD experiment. The power spectra are normalized with respect to the maximum of the received signal spectrum.

the delayed sliding-window RLS (SRLSd) algorithm [8] for the SI channel estimation. The SRLSd algorithm estimates the channel in the same way as the classical SRLS algorithm. The only difference is that the channel estimates are applied to the delayed inputs of the adaptive filter to provide a better tracking performance in time-varying channels [8]. The adaptive filter length is $L = 100$ taps, which corresponds to a delay spread of 25 ms (the baseband sampling rate is f_d = 4 kHz). The sliding window length is $M = 1401$. The SRLSd algorithm is also used for the first iteration of the far-end channel estimation. The filter length is $L_{\text{far}} = 20$ taps (5 ms) and the sliding window length is $M = 1401$. The reason for using such a long sliding window is to reduce the error due to the high-level residual SI.

Before the second iteration of SIC, an estimate of the far-end signal is reconstructed and removed from the received signal. At the second iteration, the homotopy SRLS-L-DCD (HSRLS-L-DCD) algorithm [9] is used for SIC due to its good tracking performance. The parameters of the algorithm are as follows: $M = 1001$, the number of basis functions (Legendre polynomials) is $P = 2$, the regularization parameter is $\tau = 0.65$, the reweighting coefficient is $\mu_w = 0.9$ and the parameter used for re-estimating the support is $\mu_d = 1.5 \times 10^{-4}$ (see details in [9]). For the far-end channel estimation, we use a shorter sliding window length $M = 1001$ compared to that used in the first iteration as the residual SI level is significantly reduced.

The averaged magnitude of the near-end and far-end channel impulse responses are shown in Fig. 4. It can be seen in Fig. 4 (a) that the multipath structure of the SI channel estimate is much clearer after the second iteration. This demonstrates that both the SI and far-end channel estimation performance are significantly improved at the second iteration.

C. Demodulation performance

To obtain the demodulation performance at various far-end SNRs, complex-valued Gaussian random noise with variance σ_n^2 is added to the baseband received signal in both half-duplex and FD experiments, where σ_n^2 is computed as: $\sigma_n^2 = (P_s - P_n)/\text{SNR} - P_n$, where P_s and P_n is the average power of the baseband far-end signal and background noise in the half-duplex experiment, respectively.

The BER performance of the receiver in half-duplex and FD lake experiments with extra additive noise is shown in Fig. 5. After the first iteration, the performance loss in the FD experiment is around 3.5 dB compared to the half-duplex case. This gap is reduced to 2 dB when the second iteration is applied. Such reduction is observed at high far-end SNRs when there is a high impact of the far-end signal on the near-end SIC performance. This demonstrates the benefit of using two iterations in FD UWA systems. Another conclusion is that the proposed FD UWA system shows a good demodulation performance close to that of the half-duplex counterpart.

In Fig. 6, we show the power spectra of the baseband signals in the experiments. The residual signals are obtained after subtracting SI and far-end signal estimates from the received signal in the FD experiment. To provide a clearer view, all the curves are smoothed by averaging over a frequency interval of 5 Hz. Here we consider a far-end SNR of 9 dB. After the first iteration, the residual signal level is about 5 to 10 dB higher than the noise floor. After the second iteration, the residual signal is reduced almost to the noise floor.

IV. Conclusions

In this paper, an FD UWA system with two iterations has been proposed. By performing the near-end SIC and far-end data demodulation in an iterative way, the influence of the far-end signal on the SIC performance has been reduced. The FD UWA system performance has been investigated in a lake experiment. With a rate 1/4 convolutional code, the loss in the detection performance in the FD experiment was about 2 dB compared to the half-duplex case.

REFERENCES

[1] M. Stojanovic and J. Preisig, "Underwater acoustic communication channels: Propagation models and statistical characterization," *IEEE Communications Magazine*, vol. 47, no. 1, pp. 84–89, 2009.

[2] J. I. Choi, M. Jain, K. Srinivasan, P. Levis, and S. Katti, "Achieving single channel, full duplex wireless communication," in *the 16th Annual International Conference on Mobile Computing and Networking, Chicago, Illinois, USA*, 2010, pp. 1–12.

[3] M. Duarte and A. Sabharwal, "Full-duplex wireless communications using off-the-shelf radios: Feasibility and first results," in *the 44th Asilomar Conference on Signals, Systems and Computers, Pacific Grove, California, USA*, 2010, pp. 1558–1562.

[4] M. Jain, J. I. Choi, T. Kim, D. Bharadia, S. Seth, K. Srinivasan, P. Levis, S. Katti, and P. Sinha, "Practical, real-time, full duplex wireless," in *the 17th Annual International Conference on Mobile Computing and Networking, Las Vegas, Nevada, USA*, 2011, pp. 301–312.

[5] M. Duarte, C. Dick, and A. Sabharwal, "Experiment-driven characterization of full-duplex wireless systems," *IEEE Transactions on Wireless Communications*, vol. 11, no. 12, pp. 4296–4307, 2012.

[6] G. Qiao, S. Gan, S. Liu, L. Ma, and Z. Sun, "Digital self-interference cancellation for asynchronous in-band full-duplex underwater acoustic communication," *Sensors*, vol. 18, no. 6, pp. 1700–1716, 2018.

[7] G. Qiao, S. Gan, S. Liu, and Q. Song, "Self-interference channel estimation algorithm based on maximum-likelihood estimator in in-band full-duplex underwater acoustic communication system," *IEEE Access*, vol. 6, pp. 62 324–62 334, 2018.

[8] L. Shen, Y. Zakharov, B. Henson, N. Morozs, and P. D. Mitchell, "Adaptive filtering for full-duplex UWA systems with time-varying self-interference channel," *IEEE Access*, vol. 8, pp. 187 590–187 604, 2020.

[9] L. Shen, Y. Zakharov, L. Shi, and B. Henson, "BEM adaptive filtering for SI cancellation in full-duplex underwater acoustic systems," *Signal Processing*, vol. 191, pp. 108 366–108 378, 2022.

[10] L. Shen, B. Henson, Y. Zakharov, and P. Mitchell, "Digital self-interference cancellation for full-duplex underwater acoustic systems," *IEEE Transactions on Circuits and Systems II: Express Briefs*, vol. 67, no. 1, pp. 192–196, 2019.

[11] L. Shen, B. Henson, Y. Zakharov, and P. D. Mitchell, "Adaptive nonlinear equalizer for full-duplex underwater acoustic systems," *IEEE Access*, vol. 8, pp. 108 169–108 178, 2020.

[12] S. Li and R. D. Murch, "Full-duplex wireless communication using transmitter output based echo cancellation," in *IEEE Global Telecommunications Conference-GLOBECOM, Houston, Texas, USA*, 2011, pp. 1–5.

[13] S. Haykin, *Adaptive Filter Theory*. Prentice Hall, 2002.

[14] J. Proakis and M. Salehi, *Digital Communications*. McGraw-Hill, 2008.

[15] E. Alameda-Hernandez, D. C. McLernon, M. Ghogho, A. Orozco-Lugo, and M. Lara, "Synchronisation for superimposed training based channel estimation," *Electronics Letters*, vol. 41, no. 9, pp. 565–567, 2005.

[16] Y. V. Zakharov and A. K. Morozov, "OFDM transmission without guard interval in fast-varying underwater acoustic channels," *IEEE Journal of Oceanic Engineering*, vol. 40, no. 1, pp. 144–158, 2014.